Adaptive Ground Clearance Control for Preparation for Fall in a Wearable Assistive Device

Jiancheng Nie
Department of Mechanical Engineering
Tokyo Institute of Technology
Tokyo, Japan
nie.j.aa@m.titech.ac.jp

Ming Jiang
Department of Mechanical Engineering
Tokyo Institute of Technology
Tokyo, Japan
jiang.m.ad@m.titech.ac.jp

Andrea Botta
Department of Mechanical and Aerospace Engineering
Politecnico di Torino
Torino, Italy
andrea.botta@polito.it

Yusuke Sugahara
Department of Mechanical Engineering
Tokyo Institute of Technology
Tokyo, Japan
sugahara.y.ab@m.titech.ac.jp

Yukio Takeda
Department of Mechanical Engineering
Tokyo Institute of Technology
Tokyo, Japan
takeda.y.aa@m.titech.ac.jp

2024 IEEE 18th International Conference on Advanced Motion Control (AMC) | 979-8-3503-4281-9/24/$31.00 ©2024 IEEE | DOI: 10.1109/AMC58169.2024.10505443

***Abstract*—Reducing the risks of falls is one of the main tasks for walking assistive devices. Some elderly people who fear falls tend to lower the distance between the ground and the support tip of the assistive device (ground clearance), but it is very easy to obstruct their walking and also not good for their health by always providing support because they lose the opportunities to use their muscles. However, if the ground clearance is too large, the risk of falls would also increase. In this paper, we introduced the concept of adaptive ground clearance to adjust the ground clearance dynamically during walking so that the assistive device can always prepare for falls. First, the ground reaction forces on two feet are modeled based on the symmetry walking assumption. Thus, the vertical motion on the hip during walking can be estimated. Second, a wearable device prototype was built according to the information about hip vertical displacement. Finally, a PID position control method was implemented on the prototype, using a low-cost distance sensor to enable real-time ground clearance adjustment. This work may inspire the design of rollators and walkers to reduce the reaction time and to prepare for falls.**

***Index Terms*—Adaptive Ground Clearance, Preparation for fall, Wearable Robots, Robot-Assisted Walking**

I. Introduction

Walking aids, also called assistive devices (such as walking sticks and walkers), are commonly used by the elderly to improve stability by means of increasing the support area, thus reducing the risks of falls [1]. Healthy elderly, although with decreased strength in the lower extremity (leg) due to aging, can still react to external disturbance by performing several balance strategies, such as ankle strategy and hip strategy [2], to maintain stability during walking. Consequently, a powered/active assistive device should not override these strategies by always providing support because the elderly would rely too much on the assistive device and not use their muscle again, thus accelerating the aging of the lower extremities. Therefore, powered assistive devices should only assist as needed (AAN) for the relatively healthy elderly who are mainly in Support Level 1-2 and Care Level 1 (nursing level focused on independence in daily life and defined by the Ministry of Health Labour and Welfare Japan [3]). This means assistive devices provide support only when the users become unstable or start to use the ankle or hip balance strategy. With the consideration of AAN, current assistive devices

This work was supported by JST SPRING (Grant Number JPMJSP2106) and by JSPS KAKENHI (Grant Number 23H01326).

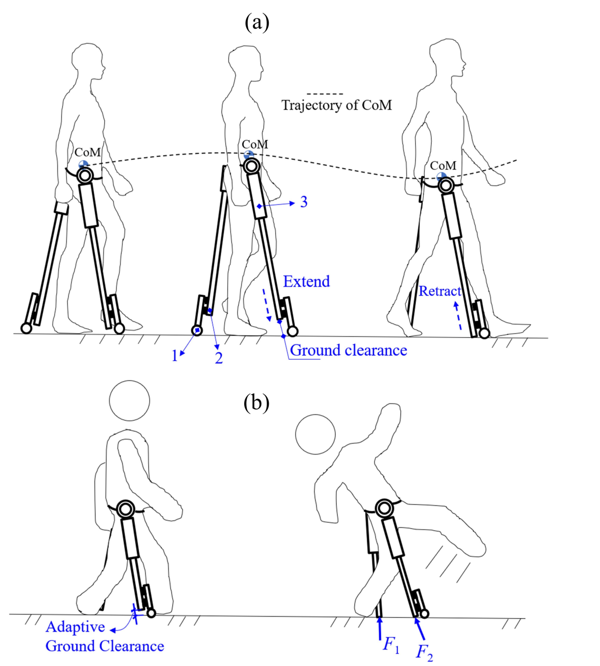

Fig. 1. The concept of adaptive ground clearance, (a) adaptive ground clearance to adapt the trajectory of the center of mass (CoM), 1 - rolling tip (passive), 2 - support tip (active), 3 - wearable robotic support limb (RSL); (b) quick response to the unstable situation based on the adaptive clearance

can be discussed. Exoskeleton robots can strengthen balance strategies by directly connecting the users' joints (ankle, hip, etc.) and providing support forces/torques. However, these reinforcements rely on good alignment between human joints and robot joints. Otherwise, the misalignment, in turn, can weaken walking stability. Thus, additional mechanism design is required for misalignment reduction [4], [5]. Cane robots are not suitable for users with limited strength in the upper limbs. Previous studies have shown that excessive use of walking sticks and crutches can cause pain and discomfort in shoulder joints because of a prolonged posture of grasping and direct pressure from the crutches [6], [7]. As for the wearable devices utilizing momentum exchanges (gyroscope or flywheel) [8] or inertial effects (robotic tail) [9], these solutions don't obstruct natural human walking and are only activated when users are facing disturbances. However, it requires considerable mass (up to 10 kg depending on rotation speed) to realize the momentum exchanges or inertial effects.

To provide a wearable device solution for the relatively healthy elderly, it must be non-obstructive and assistive as needed. In our previous research, we proposed a wearable assistive device called robotic support limb (RSL) which can make motions independently to the knee and ankle joints and does not require strength in the upper limb [10], [11]. To provide support when people become unstable, the reaction of an assistive device is time-critical. So we want to shorten the distance between the assistive device and the ground (ground clearance) as much as possible, just like the people who fear falls. However, when the ground clearance is set too small, the assistive device will inevitably obstruct human walking by always providing support (contacting the ground) even though the quick reaction for fall prevention is fulfilled in this case. On the contrary, if we set the ground clearance too large, the reaction time will increase, and the more the human body tilts, the larger the support force needed.

To tackle the trade-off problem in ground clearance, we propose a concept of adaptive ground clearance, as shown in Fig. 1. In Fig. 1 (a), the support tip can always maintain a reasonable ground clearance to prepare for unstable cases. When the hip position is raised during the stance phase of walking, the support tip can minimize the ground clearance by extension and vice versa. Thus, when the user suddenly becomes unstable, RSL can touch the ground quickly for fall prevention because the ground clearance is always kept small, as shown in Fig. 1 (b). To be clear, the passive rolling tip always contacts the ground, but it does not provide effective support force, while the support tip contacts the ground with sufficient ground reaction force only when it is needed to prevent a fall. The purpose of the rolling tip is to support the weight of RSL partially and to act as a suspension.

In the following sections of the paper, the vertical displacement of the human center of mass is analyzed so that the prototype can be designed and presented. Finally, the motion control of ground clearance is discussed and a simple experiment is demonstrated.

II. The Vertical Displacement of Human Center of Mass

Since RSL is attached to the human hip position, the vertical displacement of the hip is required for adaptive ground clearance. In this study, we assume the human center of mass (CoM) is placed around the hip. Therefore, we turn to analyze the trajectory of CoM during walking.

A. The Ground Reaction Force Estimation

It is common to use the inverted pendulum model [12], [13] for CoM tracking and controlling in humanoid robot research and human biomechanics study. Here, we use a straightforward way to analyze the CoM acceleration via ground reaction force because we only want to assess the range of excursion of CoM for the prototype design.

If we consider a left foot on the ground from the time $t = -\tau/2$ to $t = \tau/2$, then for a given time t within the interval, the vertical component of the ground reaction force $F_{z,left}$ can be approximately presented by a truncated Fourier series [14]:

$$F_{z,left} \approx a_z(\cos\frac{\pi t}{\tau} - q_z \cos\frac{3\pi t}{\tau})Mg \tag{1}$$

where a_z is a scale factor and q_z is known as the shape factor. Usually, for human walking, the value of the shape factor is equal to or greater than 0.2 and enlarges with the increase of walking speed [15]. Therefore, we select a set value of 0.2, 0.3, and 0.4 for q_z to simulate the slow, normal, and fast walking speed conditions. The coefficient a_z is a constant value [14], and we select a value of 1 for all three walking conditions in this study. M is the human body mass and g is the acceleration of gravity.

In the single support phase, the duration of the stance leg contacting the ground is around $0.4T$, where T is the gait cycle. And the duration of the double support phase is around $0.2T$. Therefore, the period of a foot on the ground is

$$\tau = 0.4T + 0.2T = 0.6T. \tag{2}$$

In addition, based on the symmetric assumption, the ground reaction force of the right leg is the same as the left one but with a phase difference. Since the distance between the left and right leg is half the stride length, the phase difference is $0.5T$ and can be converted to $5\tau/6$. Thus, the vertical component of the ground reaction force in the right leg $F_{z,right}$ can be derived as

$$F_{z,right} \approx a_z[\cos\frac{\pi}{\tau}(t - \frac{5}{6}\tau) - q_z \cos\frac{3\pi}{\tau}(t - \frac{5}{6}\tau)]Mg. \tag{3}$$

Therefore, the estimated ground reaction forces on two legs can be simulated as shown in Fig. 2 during one gait cycle under slow (q_z = 0.2), normal (q_z = 0.3), and fast walking (q_z = 0.4) conditions.

B. The Vertical Displacement of CoM

Based on the estimation of ground reaction forces, the vertical human CoM acceleration $\ddot{z}$ can be expressed as:

$$\ddot{z} = \frac{F_{z,left} + F_{z,right} - Mg}{M}. \tag{4}$$

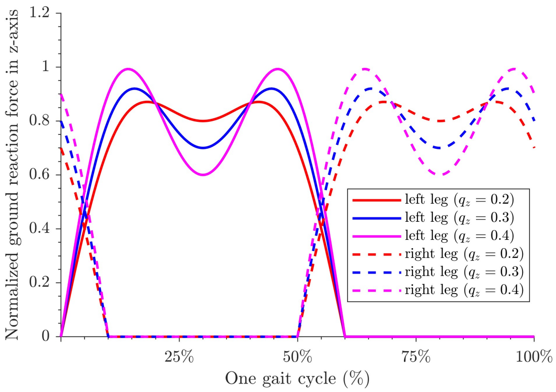

Fig. 2. The estimated ground reaction forces in the vertical z-axis against time during a gait cycle, where q_z with values of 0.2, 0.3, and 0.4 represent the slow, normal, and fast walking conditions, respectively.

Then, the vertical velocity ($\dot{z}$) and displacement (z) of human CoM can be calculated by integrating the human CoM acceleration and the vertical velocity over a period of t ($t \in$ [0, T]), respectively:

$$\begin{cases} \dot{z}(t) = \dot{z}_0 + \int_0^t \ddot{z}(\delta)\,\mathrm{d}\delta \\ z(t) = z_0 + \int_0^t \dot{z}(\delta)\,\mathrm{d}\delta \end{cases} \tag{5}$$

where $\dot{z}_0$ is the initial value representing the vertical CoM velocity at the beginning of the gait cycle, and we select it as a value of 0. Similarly, z_0 is the initial integration value for the vertical CoM position at the beginning of the gait cycle, and it is set as 0.9 m. Here, 0.9 m is just the initial state of the vertical COM position and we are more concerned about the relative distance between the initial and current COM displacement.

Consequently, the vertical velocity and displacement of human CoM can be calculated and shown in Fig. 3 according to the initial conditions.

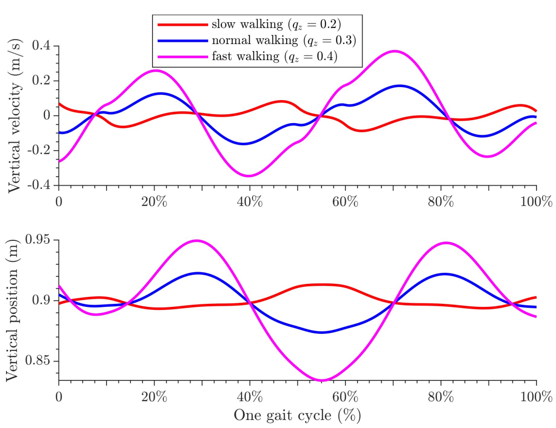

Fig. 3. The vertical velocity ($\dot{z}(t)$) and displacement ($z(t)$) are simulated at three different walking conditions (slow, normal and fast speeds) during one gait cycle.

The vertical excursion of human CoM is defined as the subtraction of maximum and minimum values in the vertical displacement waveform. Fig. 3 shows that the value of human CoM excursion becomes greater as the walking speed increases, which is consistent with the studies [16], [17] where they used the reflective markers and force plates to measure the human CoM displacement. In addition, the simulated vertical excursions in slow and normal walking conditions (20 mm and 50 mm, respectively) are comparable with the results in [16] where the vertical excursions were 27.4 ± 5.2 mm (at the speed of 0.7 m/s) and 48.3 ± 9.2 mm (at the speed of 1.6 m/s). As for the simulated fast-walking condition, the vertical excursion is 120 mm. We didn't find the actual corresponding walking speed in the references because the maximum recorded walking speed is 1.6 m/s [16], [17].

III. The Physical Prototype

To build a prototype realizing the concept of adaptive ground clearance, the requirements of support tip velocity and range of motion are needed. From the above analysis of human CoM displacement, the vertical velocity and displacement around the hip range from 0.07 m/s to 0.17 m/s and 20 mm to 50 mm between slow and normal walking conditions, respectively. In addition, since the targeted users are relatively healthy elderly and their walking speeds are usually slow (ranging from 0.9 m/s -1.3 m/s [18], [19]), we focus on the slow speed condition to build a prototype for the proof-of-concept. Therefore, the requirements for the design of the RSL support tip are determined:

- **Velocity**: the velocity of the active support tip should be larger or equal to 0.1 m/s.
- **Range of motion**: The range of motion of RSL in the support limb direction should be more than 40 mm.

Therefore, two 3-DoF (degree of freedom) support limbs are built accordingly and connected to a wearable interface that is mounted on the human hip, as shown in Fig. 4. Two rotational DoFs (1st and 2nd) are driven by gear transmission and pulley-belt mechanism, respectively. The 3rd DoF (prismatic joint) consists of one 1:2 timing belt and another 1:1 timing belt as well as a linear guide (ZLW-0630, igus, Germany), driven by a servo motor (Dynamixel MX-64T, ROBOTIS, South Korea). Besides the above-mentioned design requirements, some design considerations are summarized as follows:

- **Compact design**: Two synchronous timing belts in the 3rd DoF are transmitted via an idler pulley so that the pulley of the 3rd DoF can share the same axis with that of the 2nd DoF.
- **Triangle-shaped reinforcing frame**: To bear and withstand the reaction force from the limb direction, a triangle-shaped reinforcing frame is used between the support limb and wearable interface, fixed by two bearings on the wearable interface.
- **Motor placement**: Instead of placing near the joints, the motors for the 2nd and 3rd DoFs are placed on the top of the triangle-shaped reinforcing frame and are in line with the axis of the 1st DoF. This minimizes the inertial effects from the 2nd and 3rd DoFs when the 1st DoF rotates.

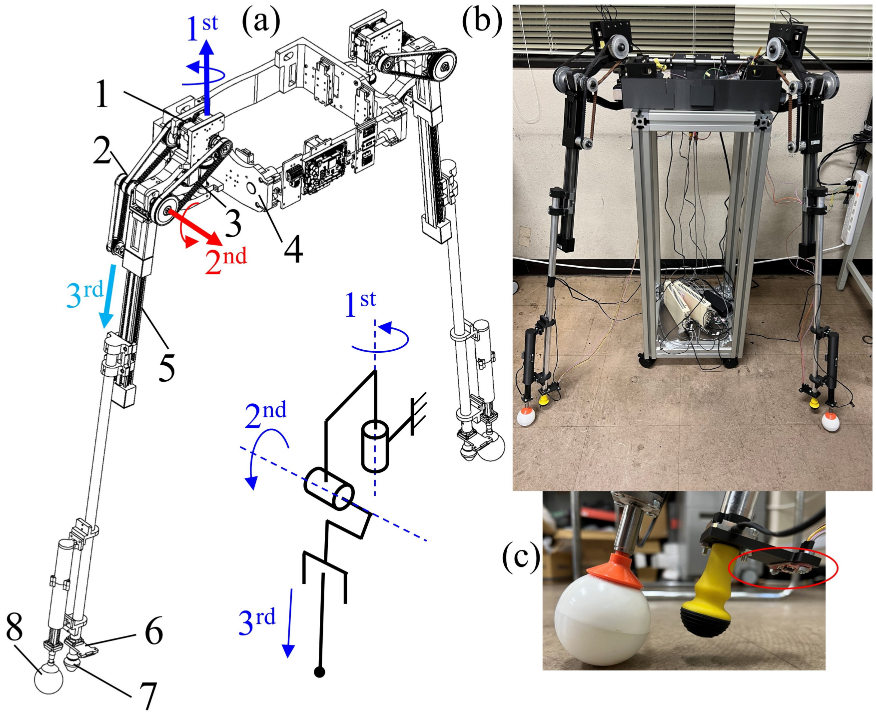

Fig. 4. The physical prototype of RSL, (a) 3D CAD model, 1 - servo motor, 2 - idler pulley, 3 - timing belt, 4 - wearable interface, 5 - linear guide, 6 - distance sensor, 7 - support tip, 8 - passive rolling tip; (b) the physical prototype; (c) support tip and distance sensor

In practice, this prototype can reach a velocity of 0.10 m/s and has a stroke of 200 mm in the limb axis (prismatic joint), which fulfills the design requirements.

IV. ADAPTIVE GROUND CLEARANCE CONTROL

A PID position controller is applied to achieve an adaptive ground clearance to prepare for falls during human walking. First, a low-cost distance sensor (VL6180x, SparkFun Electronics, USA) is selected and controlled by a microcontroller (OpenCR1.0, ROBOTIS, South Korea) via I^2C communication. The distance sensor is a time-of-flight sensor (measuring the time between reflective distances) with a range of 100 mm, which is mounted on the support tip, and can move with the support tip, as shown in Fig. 4 (c).

Second, the set point (x_d) needs to be determined. The set point (x_d) is the desired value, and by controlling the distance sensor measurement (x), we can achieve the needed ground clearance (d). Due to the incline (inclination α) of RSL, the relationship between the measurement of distance sensor (x) and ground clearance (d) is described as

$$x = \frac{d}{\cos\alpha} + a \tag{6}$$

where a is the length of the support tip as shown in Fig. 5 (a).

In addition, a previous study of the elderly fall time showed that the average fall duration (from the beginning of the descent to pelvis impact) was 583 ms [20]. Considering that fall detection also needs time, we selected the ground clearance (d) as 25 mm, equal to around half of the fall duration at the speed of 0.1 m/s.

Therefore, the set point(x_d) is determined as 50 mm based on the ground clearance (25mm) and (6). The schematic of the PID controller can be shown in Fig. 5 (b). The control signal (u, output of PID controller) is a position value referred to another motor controller which is not shown in Fig. 5.

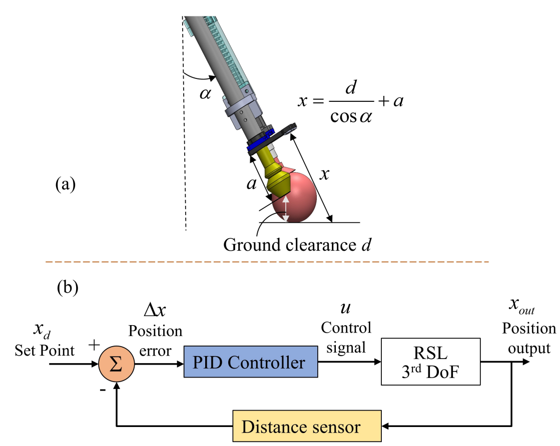

Fig. 5. The Schematic of PID position control method, (a) the relationship between the measurement of distance sensor (x) and ground clearance (d); (b) PID controller, the set point (x_d) is the desired position and x_{out} is the actual value measured by the distance sensor.

Third, to test the performance of the controller, we conducted experiments that simulated the change of ground clearance by using a cover or tilting the aluminum frame where the prototype is placed on the top of the frame. The purpose of the experiments was to show the preparation for falling through adaptive clearance control, not experiments for demonstrating how to react to a fall. When the cover approaches and blocks the field of view of the distance sensor, the distance measurement (x) becomes smaller than 50 mm (set point). Immediately (with a response time of 225 ms), the support limb will retract to maintain the desired distance. Similarly, when the cover is removed, the support limb will extend the corresponding distance. This result can be seen in Fig. 6.

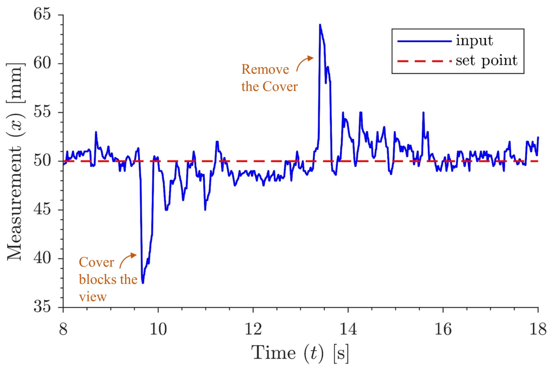

Fig. 6. The results of initial simulated experiments

V. Discussion and Future Work

This paper presents a concept of adaptive ground clearance control for preparation for falls. Although nothing may happen in normal walking, we can do some preparations through the measurement or estimation of human-environment interaction, like ground clearance. A method to model the ground reaction forces is proposed, and the simulation results of CoM vertical displacement match those measurements obtained by reflective markers and force plates. Initial simulated experiments verify the concept of adaptive ground clearance on a wearable RSL prototype. However, it can be found the noise of distance measurements in Fig. 6. Although we have used a window size of 100 ms to average the signal (a simple type of average filter), the improvement seems limited. Here, the measurement cycle is five times faster than the control cycle, and we average the reading by summarizing the five measurements in 100 ms. We consider designing a more effective low pass filter or choosing another distance sensor in the subsequent study. We should avoid using such a window size to process the data despite the short period (around 1/5 of the fall duration) because the reaction will be delayed if an unstable situation happens within this period. Besides, more versatile simulated or human experiments are considered to continue the evaluation of adaptive ground clearance and its effects on human users.

In future work, we plan to explore fall prediction, which can help the RSL system better prepare for falls. In addition, we also consider designing a more robust and compliant controller for preparation for falls and reaction to falls. In hardware design, it should be a mechanism with variable stiffness adaptive to normal walking and fall prevention. In software design, we plan to focus on quick response and how to shift the control mode between normal walking and fall prevention with proper fall prediction. Experimental investigations considering the actual use scenarios will be conducted based on the above.

References

[1] M. W. Whittle, Gait analysis: an introduction. Butterworth-Heinemann, 2014.

[2] B. Stephens, "Humanoid push recovery," in 2007 7th IEEE-RAS International Conference on Humanoid Robots, pp. 589-595, 2007.

[3] "Definition and procedure for certification of the need for long-term care," https://www.mhlw.go.jp/file/05-Shingikai-11901000-Koyoukintoujidoukateikyoku-Soumuka/0000126240.pdf. accessed November 8, 2023 (In Japanese).

[4] T. Kim, M. Jeong, and K. Kong, "Bioinspired knee joint of a lower-limb exoskeleton for misalignment reduction," IEEE/ASME Transactions on Mechatronics, vol. 27, no. 3, pp. 1223-1232, 2022.

[5] H. Li, et al., "Mechanical compliance and dynamic load isolation design of lower limb exoskeleton for locomotion assistance," IEEE/ASME Transactions on Mechatronics, vol. 27, no. 6, pp. 5392-5402, 2022.

[6] K. J. Mcquade, M. Finley and A. S. Oliveira, "Upper extremity joint stresses during walker-assisted ambulation in post-surgical patients," Brazilian Journal of Physical Therapy, vol. 15, pp. 332–337, 2011.

[7] N. B. Jain, L. D. Higgins, J. N. Katz and E. Garshick, "Association of shoulder pain with the use of mobility devices in persons with chronic spinal cord injury," PM&R, vol. 2, pp. 896–900, 2010.

[8] D. Lemus, J. van Frankenhuyzen, and H. Vallery, "Design and evaluation of a balance assistance control moment gyroscope," Journal of Mechanisms and Robotics, vol. 9, no. 5, pp. 051007, 2017.

[9] A. Maekawa, K. Kawamura, and M. Inami, "Dynamic assistance for human balancing with inertia of a wearable robotic appendage," In 2020 IEEE/RSJ International Conference on Intelligent Robots and Systems (IROS), pp. 4077-4082), 2020.

[10] J. Nie, Y. Sugahara, and Y. Takeda, "Design of Wearable Robotic Support Limbs for Walking Assistance Based on Configurable Support Polygon," In 2022 IEEE 3rd International Conference on Human-Machine Systems (ICHMS), pp. 1-6, 2022.

[11] J. Nie, M. Jiang, A. Botta, and Y. Takeda, "An adaptive gait event detection method based on stance point for walking assistive devices," Sensors and Actuators A: Physical, vol. 364, 114842, 2023.

[12] S. Kajita, F. Kanehiro, K. Kaneko, K. Yokoi, and H. Hirukawa, " The 3D linear inverted pendulum mode: A simple modeling for a biped walking pattern generation," In Proceedings 2001 IEEE/RSJ International Conference on Intelligent Robots and Systems. Expanding the Societal Role of Robotics in the the Next Millennium, Vol. 1, pp. 239-246, 2001.

[13] A. Wu and H. Geyer, "The 3-D spring–mass model reveals a time-based deadbeat control for highly robust running and steering in uncertain environments," IEEE Transactions on Robotics, vol. 29, no. 5, pp. 1114-1124, 2013.

[14] R. M. Alexander, "Bipedal animals, and their differences from humans," Journal of anatomy, vol. 204, no. 5, pp. 321-330, 2004.

[15] R. M. Alexander, "Optimization and gaits in the locomotion of vertebrates," Physiological reviews, vol. 69, no. 4, pp. 1199-1227, 1989.

[16] M. S. Orendurff, A.D. Segal, G. K. Klute, J. S. Berge, E. S. Rohr, and N. J. Kadel, "The effect of walking speed on center of mass displacement," Journal of Rehabilitation Research and Development, vol. 41, no. 6, 2004.

[17] S. A. Gard, S. C. Miff, and A. D. Kuo, "Comparison of kinematic and kinetic methods for computing the vertical motion of the body center of mass during walking," Human movement science, vol. 22, no. 6, pp. 597-610, 2004.

[18] R. W. Bohannon, "Comfortable and maximum walking speed of adults aged 20—79 years: reference values and determinants," Age and ageing, vol. 26, no. 1, pp. 15-19, 1997.

[19] J. A. Langlois, P. M. Keyl, J. M. Guralnik, D. J. Foley, R. A. Marottoli and R. B. Wallace, "Characteristics of older pedestrians who have difficulty crossing the street," American journal of public health, vol. 87, no. 3, pp. 393-397, 1997.

[20] W. J. Choi, J. M. Wakeling, and S. N. Robinovitch, "Kinematic analysis of video-captured falls experienced by older adults in long-term care," Journal of biomechanics, vol. 48, no. 6, pp. 911-920, 2015.